SIAM J. APPL. MATH.
Vol. 76, No. 4, pp. 1658–1682

DIFFUSION IN CELLS WITH STOCHASTICALLY GATED GAP JUNCTIONS*

PAUL C. BRESSLOFF†

Abstract. We analyze a one-dimensional (1D) model of molecules diffusing along a line of N cells that are connected via stochastically gated gap junctions. Each gate switches between an open ($n = 0$) and a closed ($n = 1$) state according to a two-state Markov process, and the gates are treated as statistically independent. We proceed by spatially discretizing the stochastic diffusion equation using finite differences and constructing the Chapman–Kolmogorov (CK) equation for the resulting finite-dimensional stochastic hybrid system. We thus generate a hierarchy of equations for the rth-order moments of the stochastic concentration, which in the continuum limit take the form of r-dimensional parabolic PDEs. We explicitly solve the first-order moment equations for $N = 2$ and calculate the effective permeability of the gap junction. For $N > 2$ (more than one gap junction), we show that the N-cell network has a completely different effective single-gate permeability when each particle (rather than each gate) independently switches between two conformational states $n = 0, 1$ and can only pass through a gate when $n = 0$. This difference is due to the fact that for switching gates, all particles diffuse in the same random environment, resulting in nontrivial statistical correlations. In both cases, the effective single-gate permeability has a nontrivial dependence on the number of cells N.

Key words. gap junctions, diffusion, piecewise deterministic PDEs, channel permeability

AMS subject classifications. 82C31, 92C37, 35R60, 92C20

DOI. 10.1137/15M1045818

1. Introduction.

Gap junctions are arrays of transmembrane channels that connect the cytoplasm (aqueous interior) of two neighboring cells and thus provide a direct diffusion pathway between the cells. Cells sharing a gap junction channel each provide a hemichannel (also known as a connexon) that connect head-to-head [10, 37, 18]; see Figure 1. Each hemichannel is composed of proteins called connexins that exist as various isoforms named Cx23 through Cx62, with Cx43 being the most common. The physiological properties of a gap junction, including its permeability and gating characteristics, are determined by the particular connexins forming the channel. Gap junctions have been found in almost all animal organs and tissues and allow for direct electrical and chemical communication between cells. Electrical coupling is particularly important in cardiac muscle, where the signal to contract is passed efficiently through gap junctions, allowing the heart muscle cells to contract in unison. Gap junctions (or electrical synapses) are also present throughout the central nervous system, including the neocortex and hippocampus [6]. Direct chemical communication between cells occurs through the transmission of small second messengers such as inositol triphosphate (IP3) and calcium (Ca^{2+}). More generally, gap junctions allow small diffusing molecules to undergo cytoplasmic transfer between cells, whereas large biomolecules such as nucleic acids and proteins are blocked. One example of long-range chemical signaling via gap junctions is the propagation of intercellular Ca^{2+} waves (ICWs), which consist of increases in cytoplasmic Ca^{2+} concentration that are

*Received by the editors October 28, 2015; accepted for publication (in revised form) June 2, 2016; published electronically August 24, 2016.
http://www.siam.org/journals/siap/76-4/M104581.html
Funding: The research of the author was supported by the National Science Foundation (DMS-1120327).
†Department of Mathematics, University of Utah, Salt Lake City, UT 84112 (bressloff@math.utah.edu).

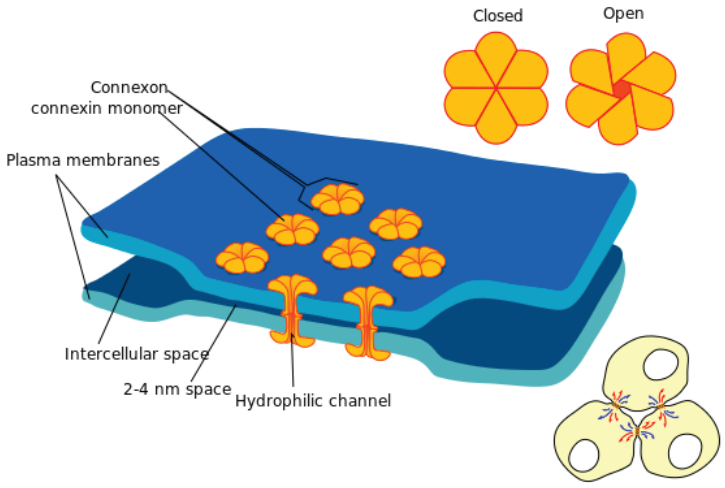

FIG. 1. *Schematic diagram of gap junction coupling between two cells. (Mariana Ruiz/Wikimedia Commons/Public Domain, https://commons.wikimedia.org/wiki/File:Gap_cell_junction-en.svg.)*

communicated between cells and appear as waves that spread out from an initiating or trigger cell [7, 38, 40, 26, 27]. An ICW often propagates at a speed of 10–20 μm/s and lasts for periods of up to tens of seconds, indicating that it can involve the recruitment of hundreds of contiguous cells. Indeed, it has been hypothesized that ICWs in glial cells known as astrocytes could provide a potential mechanism for coordinating and synchronizing the activity of a large group of neurons via the so-called tripartite synapse [40, 26].

Just as with the opening and closing of ion channels, gap junctions can be gated by both voltage and chemical agents. There appear to be at least two gating mechanisms associated with gap junctions [4], as illustrated in Figure 2. The first involves a fast gate located at the cytosplasmic entrance of a hemichannel, which has

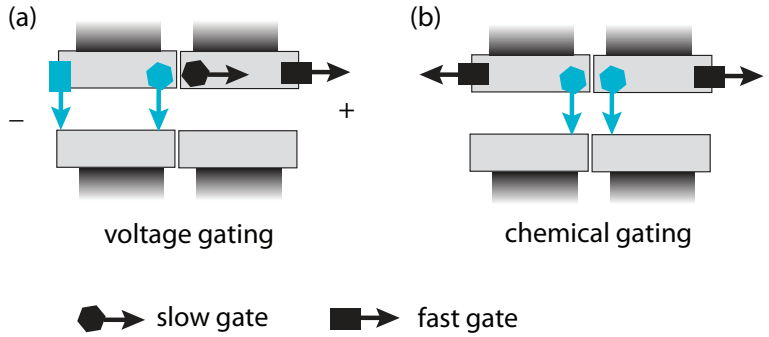

FIG. 2. *Schematic illustration of a Cx43 gap junction channel containing fast (arrow with square) and slow (arrow with hexagon) gates.* (a) *Voltage gating is mediated by both fast and slow gating mechanisms.* (b) *Chemical gating is mediated by the slow gating mechanism in both hemichannels. (Redrawn from* [4, *Figure* 15].*)*

transition times of order 1 ms and is voltage controlled. The second is based on a slow gate located towards the center of a cell-to-cell channel (or the extracellular end of a hemichannel), which has transition times of order 10 ms and is both voltage and chemically modulated. Even when a gap junction is open, it tends to restrict the flow of molecules, and this is typically modeled by assuming that a gap junction has a certain channel permeability [21]. In this paper, we follow a different approach by treating a gap junction as a randomly fluctuating gate that switches between an open and a closed state. In particular, we consider a simple one-dimensional (1D) model of molecules diffusing along a line of N cells that are connected via $(N-1)$ stochastically gated gap junctions. Each gate switches between an open ($n=0$) and a closed ($n=1$) state according to a two-state Markov process, and the gates are treated as statistically independent. We analyze the resulting stochastic PDE by extending the recent analysis of diffusion in a bounded domain with randomly switching boundaries [2]. That is, we spatially discretize the stochastic diffusion equation using finite differences and construct the Chapman–Kolmogorov (CK) equation for the resulting finite-dimensional piecewise deterministic ODE, also known as a stochastic hybrid system [1]. We thus generate a hierarchy of equations for the rth-order moments of the stochastic concentration, which take the form of r-dimensional parabolic PDEs in the continuum limit. We explicitly solve the first-order moment equations for $N=2$ and calculate the effective permeability of the gap junction. For $N>2$ (more than one gap junction), we show that the N-cell network has a completely different effective single-gate permeability when each particle (rather than each gate) independently switches between two conformational states $n=0,1$ and can only pass through a gate when $n=0$. This difference is due to the fact that for switching gates, all particles diffuse in the same random environment, resulting in nontrivial statistical correlations. In both cases, the effective single-gate permeability has a nontrivial dependence on the number of cells N.

From a more general perspective, the role of noise in the opening and closing of membrane channels has become a major topic of interest, particularly within the context of neuronal ion channels. The membrane potential of a neuron changes as ions such as Na^+ and K^+ pass in and out of the cell through voltage-dependent channels within the membrane, and the opening and closing of the channels is stochastic due to thermal fluctuations. In classical approaches, the number of ion channels is assumed to be very large, and thus the fluctuations in membrane potential from individual stochastic channels is ignored in favor of a deterministic average. More recent work has questioned this assumption. It has been shown that channel noise indeed produces membrane potential fluctuations that are large enough to affect action potential timing [14, 5, 8, 20, 23, 17, 22, 32] and increase the range of spiking behavior exhibited in some neural populations [42], with the effects of channel noise increasing dramatically as neurons become smaller. However, even when large numbers of stochastic ion channels are present in a neuron, fluctuations can become critical near the action potential threshold [13, 39]. In addition, sodium channel noise places structural limits on neural anatomy [9], since in the case of very small neurons, significant channel noise would disrupt signal transmission [12]. In spite of the extensive interest in ion channel noise, there has been relatively little work on the effects of thermal noise on gap junction diffusive coupling, beyond modeling the voltage characteristics of a single stochastically gated gap junction [34], for example. Finally, note that in this paper we focus on steady-state solutions, where it is possible to reduce the effects of gap junctions to an effective renormalization of the diffusion coefficient. Such a simple modification is unlikely to hold for time-dependent solutions of the diffusion equation in the presence of gap junctions.

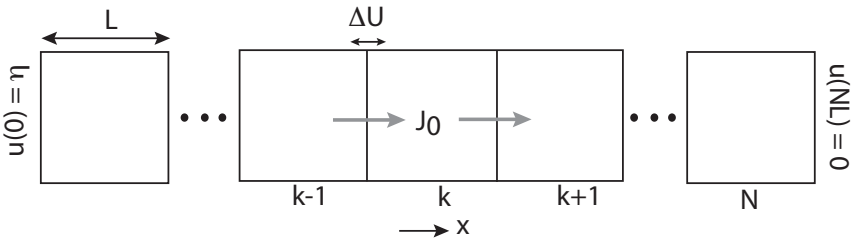

FIG. 3. *One-dimensional line of cells coupled by gap junctions. At steady-state there is a uniform flux J_0 through each cell but a jump discontinuity $\Delta U = -J_0/\mu$ in the concentration across each gap junction, where μ is the permeability of each junction. See text for details.*

2. Effective diffusion coefficient for a deterministic 1D model. Following Keener and Sneyd [21], consider a simple one-dimensional (1D) model of molecules diffusing along a line of N cells that are connected via gap junctions (see Figure 3). For simplicity, we ignore any nonlinearities arising from chemical reactions. Since gap junctions have relatively high resistance to flow compared to the cytoplasm, we assume that each intercellular membrane junction acts like an effective resistive pore with some permeability μ. Suppose that we label the cells by an integer k, $k = 1, \ldots, N$, and take the length of each cell to be L. Let $u(x,t)$ for $x \in ([k-1]L, kL)$ denote the particle concentration within the interior of the kth cell, and assume that it evolves according to the diffusion equation

$$\frac{\partial u}{\partial t} = D\frac{\partial^2 u}{\partial x^2}, \quad x \in ([k-1]L, kL),\ t > 0. \tag{2.1}$$

However, at each of the intercellular boundaries $x = l_j \equiv jL$, $j = 1, \ldots, N-1$, the concentration is discontinuous due to the permeability of the gap junctions. Conservation of diffusive flux across each boundary then implies that

$$-D\frac{\partial u(l_k^-,t)}{\partial x} = -D\frac{\partial u(l_k^+,t)}{\partial x} = \mu[u(l_k^-,t) - u(l_k^+,t)], \quad k = 1, \ldots, N-1, \tag{2.2}$$

where the $+$ and $-$ superscripts indicate that the function values are evaluated as limits from the right and left, respectively. Finally, it is necessary to specify the exterior boundary conditions at $x = 0$ and $x = NL$. We impose Dirichlet boundary conditions with $u(0,t) = \eta$ and $u(NL,t) = 0$.

In steady-state, there is a constant flux $J_0 = -DK_0$ through the system, and the steady-state concentration takes the form

$$u(x) = \begin{cases} K_0 x + \eta, & x \in [0, L), \\ K_0(x - [k-1]L) + U_k, & x \in ([k-1]L, kL),\ k = 2, \ldots, N-1, \\ K_0(x - NL), & x \in ([N-1]L, NL] \end{cases} \tag{2.3}$$

for the $N-1$ unknowns $K_0, U_k = u((k-1)L)$, $k = 2, \ldots, N-1$. These are determined by imposing the $N-1$ boundary conditions (2.2) in steady-state as follows:

$$J_0 = \mu[\eta + K_0 L - U_2] = \mu[K_0 L + U_2 - U_3] = \cdots \mu[K_0 L + U_{N-2} - U_{N-1}], \tag{2.4a}$$

$$J_0 = \mu[2K_0 L + U_{N-1}]. \tag{2.4b}$$

Rearranging equations (2.4a) gives

$$U_2 = \eta - \frac{J_0 L}{D} - \frac{J_0}{\mu}, \quad U_k = U_{k-1} - \frac{J_0 L}{D} - \frac{J_0}{\mu}, \quad k = 3, \ldots, N-1, \tag{2.5}$$

which can be iterated to give

$$U_{N-1} = \eta - (N-2) J_0 \left[\frac{L}{D} + \frac{1}{\mu} \right].$$

Since we also have

$$U_{N-1} = 2J_0 \left[\frac{L}{D} + \frac{1}{\mu} \right] - \frac{J_0}{\mu},$$

it follows that

$$J_0 = \frac{D\eta}{NL} \left[1 + \frac{D(N-1)}{\mu L N} \right]^{-1}. \tag{2.6}$$

Introducing the effective diffusion coefficient D_e according to

$$J_0 = \frac{D_e \eta}{NL}, \tag{2.7}$$

we see that for large N,

$$\frac{1}{D_e} = \left[\frac{1}{D} + \frac{1}{\mu L} \right]. \tag{2.8}$$

3. A pair of cells coupled by a stochastically gated gap junction. In the following we will calculate the mean steady-state flux through a line of cells in which each gap junction randomly switches between an open and a closed state. We will show that the mean concentration is still given by a constant gradient with jump discontinuities at the gap junctions, but the flux is now a nontrivial function of model parameters. We start by looking at a pair of stochastically coupled cells; see Figure 4. For the sake of generality, we allow the two cells to have different lengths l and $2L - l$ with $0 < l \leq L$. The basic problem can be formulated as follows. We wish to solve the diffusion equation in the open domain $\Omega = \Omega_1 \cup \Omega_2$ with $\Omega_1 = (0, l)$ and $\Omega_2 = (l, 2L)$, with the interior boundary between the two subdomains at $x = l$ randomly switching between an open and a closed state. Let $n(t)$ denote the discrete state of the gate at time t with $n(t) = 0$ if the gate is open and $n(t) = 1$ if it is closed. Assume that transitions between the two states $n = 0, 1$ are described by the two-state Markov process,

$$0 \underset{\alpha}{\overset{\beta}{\rightleftharpoons}} 1.$$

The random opening and closing of the gate means that particles diffuse in a random environment according to the piecewise deterministic equation

$$\frac{\partial u}{\partial t} = D \frac{\partial^2 u}{\partial x^2}, \quad x \in \Omega_1 \cup \Omega_2, \ t > 0, \tag{3.1}$$

with u satisfying Dirichlet boundary conditions on the exterior boundaries of Ω,

$$u(0, t) = \eta > 0, \quad u(2L, t) = 0, \tag{3.2}$$

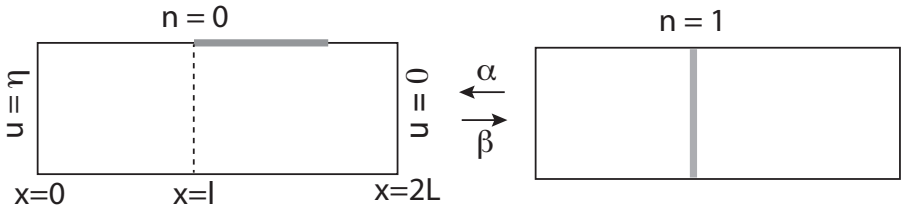

FIG. 4. *Pair of cells of length l and $2L-l$, respectively, that are coupled by a stochastically gated gap junction. The gate at $x=l$ stochastically switches between an open and a closed state according to a two-state Markov process with transition rates α, β. Dirichlet boundary conditions are imposed on the exterior boundaries.*

and $n(t)$-dependent boundary conditions on the interior boundary at $x=l$,

$$u(l^-,t)=u(l^+,t), \quad \partial_x u(l^-,t)=\partial_x u(l^+,t) \quad \text{for } n(t)=0, \tag{3.3}$$

$$\partial_x u(l^-,t)=0=\partial_x u(l^+,t) \quad \text{for } n(t)=1, \tag{3.4}$$

where $l^{\pm}=\lim_{\epsilon\to 0^+} l\pm\epsilon$. That is, when the gate is open there is continuity of the concentration and the flux across $x=l$, whereas when the gate is closed the right-hand boundary of Ω_1 and the left-hand boundary of Ω_2 are reflecting. For simplicity, we assume that the diffusion coefficient is the same in both compartments so that the piecewise nature of the solution is solely due to the switching gate. For the sake of illustration we take the exterior boundary conditions to be Dirichlet, but the analysis is easily modified in the case of a Neumann boundary condition at one of the ends, for example.

One way to analyze the above piecewise deterministic PDE is in terms of moments of the stochastic particle concentration [24, 2]. Extending our previous analysis of 1D diffusion in domains with switching exterior boundaries [2], we will derive moment equations by discretizing space and constructing the CK equation for the resulting finite-dimensional stochastic hybrid system. (Although we carry out the analysis for a single gap junction, it is straightforward to extend the analysis to multiple gap junctions, that is, $N>2$.) The first step is to spatially discretize the piecewise deterministic PDE (3.1) using a finite-difference scheme. One advantageous feature of this discretization is that the boundary conditions can be incorporated into the resulting discrete Laplacian. Introduce the lattice spacing a such that $Ma=l$ and $(Q+1)a=2L$ for integers M,Q. Set $u_j=u(aj)$, $j=0,\dots,Q+1$. Then

$$\frac{du_i}{dt}=\sum_{j=1}^{M-1}\Delta^n_{ij}u_j+\sum_{j=M+1}^{Q}\Delta^n_{ij}u_j+\eta_a\delta_{i,1},\ \eta_a=\frac{\eta D}{a^2} \tag{3.5}$$

for $i=1,\dots,M-1,M+1,\dots,Q$, and $n=0,1$ is an index indicating the state of the gate. Away from the boundaries ($i\neq 1,M\pm 1,Q$), Δ^n_{ij} is given by the discrete Laplacian

$$\Delta_{ij}=\frac{D}{a^2}[\delta_{i,j+1}+\delta_{i,j-1}-2\delta_{i,j}], \tag{3.6a}$$

with $\delta_{i,j}$ the Kronecker delta. On the left-hand exterior boundary we have $u_0=\eta$, whereas on the right-hand exterior boundary we have $u_{Q+1}=0$. On the interior boundary,

$$u_{M-2}-u^-_M=u^+_M-u_{M+2}, \quad u^+_M=u^-_M \quad \text{if } n=0$$

and

$$u_{M-2} - u_M^- = 0, \quad u_{M+2} - u_M^+ = 0 \quad \text{if } n = 1,$$

where $u_M^\pm = u_{M\pm1}$. These can be implemented by taking

$$\Delta_{1j}^n = \frac{D}{a^2}[\delta_{j,2} - 2\delta_{j,1}], \quad \Delta_{Qj}^n = \frac{D}{a^2}[\delta_{Q-1,j} - 2\delta_{Q,j}], \quad n = 0, 1, \tag{3.6b}$$

$$\Delta_{M-1,j}^0 = \frac{D}{a^2}[\delta_{M-2,j} + (\delta_{M-2,j} + \delta_{M+2,j})/2 - 2\delta_{M-1,j}], \tag{3.6c}$$

$$\Delta_{M+1,j}^0 = \frac{D}{a^2}[\delta_{M+2,j} + (\delta_{M-2,j} + \delta_{M+2,j})/2 - 2\delta_{M+1,j}], \tag{3.6d}$$

and

$$\Delta_{M\pm1,j}^1 = \frac{2D}{a^2}[\delta_{M\pm2,j} - \delta_{M\pm1,j}]. \tag{3.6e}$$

Note that when $n = 1$, the system of equations in the two compartments decouples (as expected for a closed gate).

Our spatial discretization scheme has reduced the system to a piecewise deterministic ODE known as a stochastic hybrid system [1]. Let $\mathbf{u}(t) = (u_1(t), \ldots, u_{M-1}(t), u_{M+1}(t), \ldots, u_Q(t))$ and introduce the probability density

$$\text{Prob}\{\mathbf{u}(t) \in (\mathbf{u}, \mathbf{u} + d\mathbf{u}), n(t) = n\} = p_n(\mathbf{u}, t)d\mathbf{u}, \tag{3.7}$$

where we have dropped the explicit dependence on initial conditions. The probability density evolves according to the differential CK equation [16, 1]

$$\frac{\partial p_n}{\partial t} = -\sum_{i=1}^{Q} \frac{\partial}{\partial u_i}\left[\left(\sum_{j=1, j\neq M}^{Q} \Delta_{ij}^n u_j + \eta_a \delta_{i,1}\right) p_n(\mathbf{u}, t)\right] + \sum_{m=0,1} A_{nm} p_m(\mathbf{u}, t), \tag{3.8}$$

where A is the matrix

$$A = \begin{bmatrix} -\beta & \alpha \\ \beta & -\alpha \end{bmatrix}. \tag{3.9}$$

The right-hand side consists of an advection term representing the deterministic evolution of the system in between jumps of the discrete variable, with the latter represented by the matrix A. The left nullspace of A is spanned by the vector

$$\psi = \begin{pmatrix} 1 \\ 1 \end{pmatrix}, \tag{3.10}$$

and the right nullspace is spanned by

$$\rho \equiv \begin{pmatrix} \rho_0 \\ \rho_1 \end{pmatrix} = \frac{1}{\alpha + \beta} \begin{pmatrix} \alpha \\ \beta \end{pmatrix}. \tag{3.11}$$

A simple application of the Perron–Frobenius theorem shows that the two-state Markov process with master equation

$$\frac{dP_n(t)}{dt} = \sum_{m=0,1} A_{nm} P_m(t) \tag{3.12}$$

is ergodic with $\lim_{t\to\infty} P_n(t) = \rho_n$.

Having derived the CK equation for the spatially discretized system, we can derive moment equations for the stochastic vector $\mathbf{u}(t)$ along analogous lines to our previous work [2]. Define the rth-order moments ($r \geq 1$) according to

$$v^{(r)}_{n,k_1\dots k_r}(t) = \mathbb{E}[u_{k_1}(t)\dots u_{k_r}(t)1_{n(t)=n}] = \int p_n(\mathbf{u},t)u_{k_1}(t)\dots u_{k_r}(t)d\mathbf{u}. \tag{3.13}$$

Multiplying both sides of the CK equation (3.8) by $u_{k_1}(t)\dots u_{k_r}(t)$ and integrating with respect to $\mathbf{u}$ gives (after integration by parts)

$$\frac{dv^{(r)}_{n,k_1\dots k_r}}{dt} = \sum_{s=1}^{r}\sum_{j=1,j\neq M}^{Q}\Delta^n_{k_s j}v^{(r)}_{n,k_1\dots k_{s-1}jk_{s+1}\dots k_r} + \eta_a\sum_{s=1}^{r}v^{(r-1)}_{n,k_1\dots k_{s-1}k_{s+1}\dots k_r}\delta_{k_s,1} + \sum_{m=0,1}A_{nm}v^{(r)}_{m,k_1\dots k_r}.$$

Note that we do not pick up any boundary terms when integrating by parts, since $p_n(\mathbf{u},t) \to 0$ in the limit $\mathbf{u} \to \infty$. Finally, if we retake the continuum limit $a \to 0$ with $x_s = ak_s$, we obtain a system of parabolic equations for the equal-time r-point correlations

$$C^{(r)}_n(x_1,\dots,x_r) = \mathbb{E}[u(x_1,t)u(x_2,t)\dots u(x_r,t)1_{n(t)=n}], \tag{3.14}$$

given by

$$\frac{\partial C^{(r)}_0}{\partial t} = D\sum_{s=1}^{r}\frac{\partial^2 C^{(r)}_0}{\partial x_s^2} - \beta C^{(r)}_0 + \alpha C^{(r)}_1, \tag{3.15a}$$

$$\frac{\partial C^{(r)}_1}{\partial t} = D\sum_{s=1}^{r}\frac{\partial^2 C^{(r)}_1}{\partial x_s^2} + \beta C^{(r)}_0 - \alpha C^{(r)}_1. \tag{3.15b}$$

The r-point correlations couple to the $(r-1)$-order moments via the exterior boundary conditions

$$C^{(r)}_n(x_1,\dots,x_r,t)\Big|_{x_s=2L} = 0 \tag{3.16a}$$

and

$$C^{(r)}_n(x_1,\dots,x_r,t)\Big|_{x_s=0} = \eta C^{(r-1)}_n(x_1,\dots,x_{s-1},x_{s+1},\dots,x_r,t) \tag{3.16b}$$

for $n = 0,1, s = 1,\dots,r$. Note that $C^{(0)}_n = \mathbb{E}[1_{n(t)=n}] = \rho_n$. The interior boundary conditions are

$$\Big[C^{(r)}_0(x_1,\dots,x_r,t)\Big]^{x_s=l^+}_{x_s=l^-} = 0, \quad \Big[\partial_{x_s}C^{(r)}_0(x_1,\dots,x_r,t)\Big]^{x_s=l^+}_{x_s=l^-} = 0 \tag{3.16c}$$

and

$$\partial_{x_s}C^{(r)}_1(x_1,\dots,x_r,t)\Big|_{x_s=l^-} = 0 = \partial_{x_s}C^{(r)}_1(x_1,\dots,x_r,t)\Big|_{x_s=l^+}. \tag{3.16d}$$

4. First-order moment equations and effective permeability ($N = 2$). In order to determine the effective permeability of a stochastically gated gap junction, we need to calculate the mean of the concentration $u(x,t)$,

$$\mathbb{E}[u(x,t)] = V_0(x,t) + V_1(x,t), \tag{4.1}$$

where

$$V_n(x,t) \equiv C_n^{(1)}(x,t) = \mathbb{E}[u(x,t)1_{n(t)=n}]. \tag{4.2}$$

The first-order moment equations take the form

$$\frac{\partial V_0}{\partial t} = D\frac{\partial^2 V_0}{\partial x^2} - \beta V_0 + \alpha V_1, \tag{4.3a}$$

$$\frac{\partial V_1}{\partial t} = D\frac{\partial^2 V_1}{\partial x^2} + \beta V_0 - \alpha V_1 \tag{4.3b}$$

for $x \in \Omega_1 \cup \Omega_2$, with exterior boundary conditions

$$V_0(0,t) = \rho_0\eta, \quad V_1(0,t) = \rho_1\eta, \quad V_0(2L,t) = V_1(2L,t) = 0 \tag{4.4}$$

and interior boundary conditions

$$V_0(l^-,t) = V_0(l^+,t), \ \ \partial_x V_0(l^-,t) = \partial_x V_0(l^+,t), \ \ \partial_x V_1(l^-,t) = 0 = \partial_x V_1(l^+,t). \tag{4.5}$$

To see why these are the correct boundary conditions, note that if $n(t) = n$ and $x = 0$, then $u(0,t) = \eta$ with probability one, and thus

$$V_n(0,t) = \mathbb{E}[u(0,t)1_{n(t)=n}] = \eta\mathbb{P}(n(t) = n) = \eta\rho_n.$$

Deriving the other boundary conditions is similar. (Note that the problem of diffusion in a domain with a switching interface has also recently been considered by Lawley and Keener [25]. However, they focus on the fast switching limit rather than the steady-state solution for arbitrary switching rates and do not consider the multi-interface case.)

Since equations (4.3a) and (4.3b) have a globally attracting steady-state, it follows that

$$\lim_{t\to\infty} \mathbb{E}[u(x,t)] = V(x) \equiv \sum_{n=0,1} V_n(x), \tag{4.6}$$

where $V_n(x) \equiv \lim_{t\to\infty} V_n(x,t)$. From the interior boundary conditions (4.5), we set

$$\partial_x V_0(l^-) = \partial_x V_0(l^+) = K_0,$$

with K_0 to be determined later by imposing $V_0(l^-) = V_0(l^+)$. Adding equations (4.3a) and (4.3b) then gives

$$\frac{d^2V}{dx^2} = 0, \quad x \in [0,l), \quad V(0) = \eta, \quad \partial_x V(l^-) = K_0 \tag{4.7}$$

and

$$\frac{d^2V}{dx^2} = 0, \quad x \in (l,2L], \quad \partial_x V(l^+) = K_0, \quad V(2L) = 0. \tag{4.8}$$

This yields the piecewise linear solution

$$V(x) = \begin{cases} K_0 x + \eta, & x \in [0, l), \\ K_0(x - 2L), & x \in (l, 2L]. \end{cases} \tag{4.9}$$

Since $V_0 = V - V_1$, we can rewrite (4.3b) as

$$D\frac{d^2V_1}{dx^2} - (\alpha + \beta)V_1(x) = -\beta V(x), \tag{4.10}$$

with $V_1(0) = \rho_1\eta, V_1(2L) = 0$, and $\partial_x V_1(l^-, t) = 0 = \partial_x V_1(l^+, t)$. Substituting for $V(x)$ using (4.9), we obtain a piecewise solution of the form

$$V_1(x) = B\sinh(\xi x) + \rho_1(K_0 x + \eta), \quad x \in [0, l), \tag{4.11a}$$

$$V_1(x) = C\sinh([2L - x]\xi) + \rho_1 K_0(x - 2L), \quad x \in (l, 2L], \tag{4.11b}$$

with $\xi = \sqrt{(\alpha + \beta)/D}$. We have imposed the exterior boundary conditions. The interior boundary conditions for V_1 then determine the coefficients B, C in terms of K_0 so that we find

$$V_1(x) = -\frac{\rho_1 K_0}{\xi}\frac{\sinh(\xi x)}{\cosh(\xi l)} + \rho_1(K_0 x + \eta), \quad x \in [0, l), \tag{4.12a}$$

$$V_1(x) = \frac{\rho_1 K_0}{\xi}\frac{\sinh(\xi[2L - x])}{\cosh(\xi[2L - l])} + \rho_1 K_0(x - 2L), \quad x \in (l, 2L]. \tag{4.12b}$$

Finally, we determine the unknown K_0 by requiring that $V_0(x)$ be continuous across $x = l$, that is,

$$K_0 l + \eta - V_1(l^-) = K_0(l - 2L) - V_1(l^+),$$

which yields the result

$$\frac{\rho_1 K_0}{\xi}\left[\tanh(\xi[2L - l]) + \tanh(\xi l)\right] = -\rho_0(\eta + 2K_0 L),$$

which can be rearranged to yield the following result for the mean flux through the gate, $J_0 = -DK_0$:

$$J_0 = \frac{D\eta}{2L}\frac{1}{1 + (\rho_1/\rho_0)(2\xi L)^{-1}\left[\tanh(\xi[2L - l]) + \tanh(\xi l)\right]}. \tag{4.13}$$

Comparison with (2.6) for $N = 2$ and $l = L$ implies that the stochastically gated gap junction has the effective permeability μ_e with

$$\frac{1}{\mu_e} = \frac{2\rho_1}{\rho_0}\frac{\tanh(\xi L)}{\xi D}. \tag{4.14}$$

It is useful to note some asymptotic properties of the solution given by (4.9) and (4.13). First, in the fast switching limit $\xi \to \infty$, we have $J_0 \to \eta D/2L$, $\mu_e \to \infty$, and (4.9) reduces to the continuous steady-state solution

$$V(x) = \frac{\eta(2L - x)}{2L}, \quad x \in [0, 2L].$$

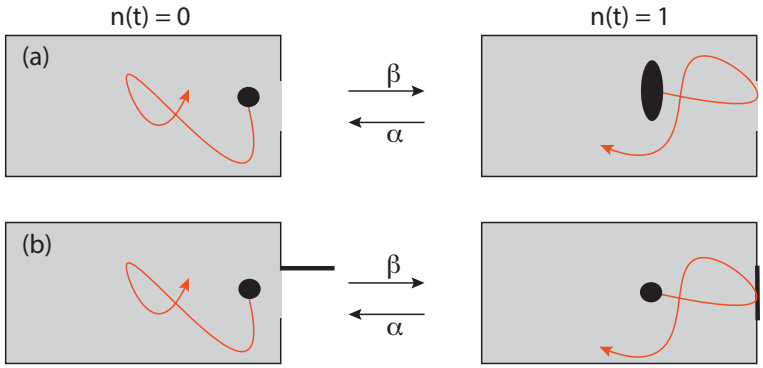

FIG. 5. *Two distinct mechanisms for stochastic gating.* (a) *Each particle switching conformational states* (b) *the physical gate switching between open and closed states.*

The mean flux through the gate is the same as the steady-state flux without a gate. On the other hand, for finite switching rates, the mean flux J_0 is reduced. In the limit $\alpha \to 0$ (gate always closed), $J_0 \to 0$ so that $V(x) = \eta$ for $x \in [0, l)$ and $V(x) = 0$ for $x \in (l, L]$. Finally, in the limit $l \to 2L$ we recover the following result for 1D diffusion in a single domain with a switching external boundary [24, 2]:

$$V(x) = \eta \frac{2L - x}{2L} \frac{1}{1 + (\rho_1/\rho_0)(2\xi L)^{-1} \tanh(2\xi L)}. \tag{4.15}$$

A few remarks are in order.

(i) In the case of a single gate the first-moment equations (4.3a) and (4.3b) have an alternative interpretation in terms of a two-population model describing the diffusion of noninteracting molecules that can independently exist in two conformational states $n = 0, 1$; molecules can only pass through the gap junction in state $n = 0$. In other words, the individual particles randomly switch between states rather than the gap junction physically opening and closing. This is illustrated in Figure 5. There is no longer a stochastic PDE since the individual particles are statistically independent (law of large numbers), and $V_n(x, t)$ is interpreted as the concentration of particles in state n at time t. On the other hand, higher-order correlations exist for a stochastic gate, since all molecules move in the same random environment. In the case of multiple gates there are significant differences between the particle and gate perspectives even at the first-moment level, as we demonstrate in section 5.

(ii) In the above analysis we calculated the average steady-state concentration and the associated steady-state flux. A particular realization of the two-cell model will have statistical fluctuations about the mean, which are characterized by the higher-order moment equations (3.15a,b) for $N = 2$. In the appendix we sketch the analysis of the steady-state two-point correlation function.

5. Multicell model. Let us return to the general case of a line of N identical cells of length L coupled by $N - 1$ gap junctions at positions $x = l_k = kL$, $1 \le k \le N - 1$; see Figure 3. We will solve the corresponding first-moment equations and calculate the steady-state flux for both switching particles and switching gates.

5.1. Switching particle perspective. We first consider the simpler case of independently switching particles. If $V_n(x, t)$ is the concentration of particles in state n, then we have the pair of PDEs given by (4.3a) and (4.3b), except now the exterior

boundary conditions are

$$V_n(0) = \rho_n \eta, \quad V_n(L) = 0, \quad n = 0, 1, \tag{5.1}$$

and the interior boundary conditions at the jth gate are

$$[V_0(x)]_{x=l_j^-}^{x=l_j^+} = 0, \quad [\partial_x V_0(x)]_{x=l_j^-}^{x=l_j^+} = 0, \tag{5.2a}$$

$$\partial_x V_1(l_j^-) = 0 = \partial_x V_1(l_j^+). \tag{5.2b}$$

Adding (4.3a) and (4.3b), we obtain the following equation for $V(x) = V_0(x) + V_1(x)$:

$$\frac{d^2V}{dx^2} = 0, \quad x \in \bigcup_{k=1}^{N} ((k-1)L, kL), \tag{5.3}$$

with exterior boundary conditions

$$V(0) = \eta, \quad V(NL) = 0$$

and interior boundary conditions

$$\partial_x V(l_j^-) = \partial_x V(l_j^+) = K_0 \quad \forall\, j = 1, \ldots, N-1.$$

It follows that $V(x)$ has the piecewise solution identical to (2.3). We thus have $N-1$ unknowns $K_0, U_2, \ldots, U_{N-1}$.

The next step is to solve (4.3b) for $V_1(x)$ with $V_0(x) = V(x) - V_1(x)$. This yields (4.10) with boundary conditions (5.1) and (5.2b). The general solution is

$$V_1(x) = \begin{cases} B_1 \sinh(\xi x) + \rho_1(K_0 x + \eta), & x \in [0, L), \\ B_k \sinh(\xi[x - [k-1]L]) + C_k \cosh(\xi[x - [k-1]L]) & \\ \quad + \rho_1[K_0(x - [k-1]L) + U_k], & x \in (l_{k-1}, l_k), \\ B_N \sinh(\xi[NL - x]) + \rho_1 K_0(x - NL), & x \in (l_{N-1}, NL], \end{cases} \tag{5.4}$$

for $k = 2, \ldots, N-1$ and $l_k = kL$. Again we have imposed the external boundary conditions. The internal boundary conditions for $V_1(x)$ then show that

$$\begin{aligned} B_1 &= -\frac{\rho_1 K_0}{\xi \cosh(\xi L)} = -B_N, \\ B_k &= -\frac{\rho_1 K_0}{\xi}, \quad k = 2, \ldots, N-1, \\ C_k &= \frac{\rho_1 K_0}{\xi} \frac{\cosh(\xi L) - 1}{\sinh(\xi L)}, \quad k = 2, \ldots, N-1. \end{aligned}$$

The $N-1$ remaining unknowns are determined by imposing continuity of $V_0(x)$ at each interior boundary as follows:

$$U_2 = K_0 L + \eta + \frac{\rho_1 K_0}{\xi \rho_0} \left[\tanh(\xi L) + \frac{\cosh(\xi L) - 1}{\sinh(\xi L)} \right], \tag{5.5a}$$

$$\begin{aligned} U_k &= U_{k-1} + K_0 L + \frac{\rho_1 K_0}{\xi \rho_0} \left[\sinh(\xi L) - \frac{[\cosh(\xi L) - 1]^2}{\sinh(\xi L)} \right], \\ &= U_{k-1} + K_0 L + \frac{2\rho_1 K_0}{\xi \rho_0} \frac{\cosh(\xi L) - 1}{\sinh(\xi L)}, \quad k = 3, \ldots, N-1, \end{aligned} \tag{5.5b}$$

$$U_{N-1} = -2K_0 L - \frac{\rho_1 K_0}{\xi \rho_0} \left[\tanh(\xi L) + \frac{\cosh(\xi L) - 1}{\sinh(\xi L)} \right]. \tag{5.5c}$$

Iterating (5.5b) and using (5.5a) yields

$$U_{N-1} = \eta + (N-2)K_0 L + (2N-5)\frac{\rho_1 K_0}{\xi\rho_0}\frac{\cosh(\xi L)-1}{\sinh(\xi L)} + \frac{\rho_1 K_0}{\xi\rho_0}\tanh(\xi L). \tag{5.6}$$

Finally, comparing (5.5c) and (5.6), we obtain the following result for the flux J_0:

$$J_0 = \frac{D\eta}{NL}\frac{1}{1+(\rho_1/\rho_0)(N\xi L)^{-1}\left[2\tanh(\xi L)+(2N-4)\dfrac{\cosh(\xi L)-1}{\sinh(\xi L)}\right]}. \tag{5.7}$$

We deduce that the effective permeability $\mu_e(N)$ in the case of N cells with $N-1$ independent, stochastically gated gap junctions is

$$\frac{1}{\mu_e(N)} = \frac{\rho_1}{[N-1]\rho_0\xi D}\left[2\tanh(\xi L)+(2N-4)\frac{\cosh(\xi L)-1}{\sinh(\xi L)}\right]. \tag{5.8}$$

This reduces to (4.14) when $N=2$. We conclude that the effective single-gate permeability is N-dependent with

$$\lim_{N\to\infty}\frac{1}{\mu_e(N)} = \frac{2\rho_1}{\rho_0\xi D}\frac{\cosh(\xi L)-1}{\sinh(\xi L)}.$$

5.2. Switching gate perspective. Now suppose that each gate independently switches between open and closed states. The discrete state of the N-cell system is represented by the binary vector $\mathbf{n} = (n_1, \ldots, n_{N-1})$, with $n_j = 0, 1$ denoting the open/closed state of the jth gate. Setting

$$V_{\mathbf{n}}(x,t) = \mathbb{E}[u(x,t)1_{\mathbf{n}(t)=\mathbf{n}}],$$

we have the system of first-order moment equations

$$\frac{\partial V_{\mathbf{n}}}{\partial t} = D\frac{\partial^2 V_{\mathbf{n}}}{\partial x^2} + \sum_{\mathbf{m}} \mathcal{A}_{\mathbf{nm}} V_{\mathbf{m}}, \tag{5.9}$$

where

$$\sum_{\mathbf{m}} \mathcal{A}_{\mathbf{nm}} V_{\mathbf{m}} = \sum_{j=1}^{N-1} A_{n_j m_j} V_{n_1,\ldots,m_j,\ldots,n_N}$$

and A is the matrix of (3.9). Equation (5.9) can be derived along similar lines to the case $N=2$ by taking first moments of the spatially discretized CK equation. The $2^{N-1}\times 2^{N-1}$ matrix $\mathcal{A}$ has a 1D nullspace spanned by the eigenvector

$$\phi_{\mathbf{n}} = \prod_{j=1}^{N-1} \rho_{n_j},$$

with ρ_n defined in (3.11). The exterior boundary conditions are

$$V_{\mathbf{n}}(0) = \phi_{\mathbf{n}}\eta, \quad V_{\mathbf{n}}(NL) = 0 \quad \forall\, \mathbf{n}, \tag{5.10}$$

and the interior boundary conditions at the jth gate are

$$[V_{\mathbf{n}}(x)]_{x=l_j^-}^{x=l_j^+} = 0, \quad [\partial_x V_{\mathbf{n}}(x)]_{x=l_j^-}^{x=l_j^+} = 0 \tag{5.11}$$

for $n_j = 0$ and

$$\partial_x V_{\mathbf{n}}(l_j^-) = 0 = \partial_x V_{\mathbf{n}}(l_j^+) \tag{5.12}$$

for $n_j = 1$.

As in the two-compartment case, we are interested in obtaining the steady-state average concentration

$$V(x) = \sum_{\mathbf{n}} V_{\mathbf{n}}(x) = \mathbb{E}[u(x)].$$

Summing the steady-state version of (5.9) over $\mathbf{n}$ and using $\sum_{\mathbf{n}} \mathcal{A}_{\mathbf{nm}} = 0$ yields

$$\frac{d^2V}{dx^2} = 0, \quad x \in \bigcup_{k=1}^{N}((k-1)L, kL), \tag{5.13}$$

with exterior boundary conditions

$$V(0) = \eta, \quad V(NL) = 0$$

and interior boundary conditions

$$\partial_x V(l_j^-) = \partial_x V(l_j^+) = K_0 \quad \forall\, j = 1, \ldots, N-1.$$

Again it follows that $V(x)$ has the piecewise solution identical to (2.3) with $N-1$ unknowns $K_0, U_2, \ldots, U_{N-1}$. These are determined by solving (5.9) for the remaining $\mathcal{N} = 2^{N-1} - 1$ moments $V_{\mathbf{n}}$, $\mathbf{n} \neq \mathbf{0}$, with $V_{\mathbf{0}} = V - \sum_{\mathbf{m}\neq\mathbf{0}} V_{\mathbf{m}}$, and imposing the boundary conditions. It is convenient to perform the change of variables

$$V_{\mathbf{n}}(x) = \phi_{\mathbf{n}} V(x) + w_{\mathbf{n}}(x), \quad \sum_{\mathbf{n}} w_{\mathbf{n}}(x) = 0. \tag{5.14}$$

Substituting the decomposition of $V_{\mathbf{n}}(x)$ into the steady-state version of (5.9) gives

$$0 = D\frac{\partial^2 w_{\mathbf{n}}}{\partial x^2} + \sum_{\mathbf{m},\mathbf{m}\neq\mathbf{0}} \widehat{\mathcal{A}}_{\mathbf{nm}} w_{\mathbf{m}}, \quad \mathbf{n} \neq \mathbf{0}, \tag{5.15}$$

with the $\mathcal{N} \times \mathcal{N}$ matrix $\widehat{\mathcal{A}}$ given by

$$\widehat{\mathcal{A}}_{\mathbf{nm}} = \mathcal{A}_{\mathbf{nm}} - \mathcal{A}_{\mathbf{n0}}. \tag{5.16}$$

The invertible matrix $\widehat{\mathcal{A}}$ has $\mathcal{N}$ real eigenpairs $(-\lambda_i, \mathbf{e}_i)$ with $\lambda_i > 0$. (This follows from the Perron–Frobenius theorem.) We can then set

$$w_{\mathbf{n}}(x) = \sum_{i=1}^{\mathcal{N}} w_i(x)\mathbf{e}_{i,\mathbf{n}}, \tag{5.17}$$

with

$$D\frac{\partial^2 w_i(x)}{\partial x^2} - \lambda_i w_i(x) = 0, \tag{5.18}$$

and exterior boundary conditions $w_i(0) = w_i(NL) = 0$. We thus obtain the piecewise solution

$$w_i(x) = \begin{cases} A_i \sinh(\xi_i x), & x \in [0, L), \\ B_{ik}\sinh(\xi_i[x - l_{k-1}]) + C_{ik}\cosh(\xi_i[x - l_{k-1}]), & x \in (l_{k-1}, l_k), \\ D_i \sinh(\xi_i(x - L)), & x \in ((N-1)L, NL], \end{cases} \tag{5.19}$$

for $i = 1, \ldots, \mathcal{N}$, $k = 2, \ldots, N-1$, and $\xi_i = \sqrt{\lambda_i/D}$. There are thus $2(N-1)\mathcal{N}$ unknown coefficients A_i, D_i, B_{ik}, C_{ik}. These can be solved in terms of the $N-1$ unknowns K_0, U_k by substituting (5.17) and (5.19) into (5.14) and imposing the $2(N-1)\mathcal{N}$ interior boundary conditions. Finally, the remaining unknowns K_0, U_j can be determined by imposing continuity of the solution $V_{\mathbf{0}}(x)$ at the $N-1$ interior boundaries $x = l_k = kL$, $k = 1, \ldots, N-1$. Although we omit the details of the algebra, it is clear that the complexity of computing the stationary flux J_0 increases significantly compared to the switching particle case, even for $N = 3$, and the resulting N-dependent effective permeability will depend on more than one coherence length ξ_i^{-1}. For the sake of illustration, we calculate the coherence lengths for $N = 3$.

Example: $N = 3$. In the case of three cells, there are four discrete states (00), (01), (10), (11), and the state transition diagram is

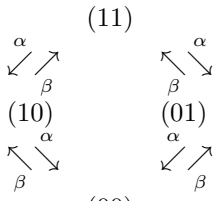

The 4×4 matrix $\mathcal{A}$ is

$$\mathcal{A} = \begin{pmatrix} -2\alpha & \beta & \beta & 0 \\ \alpha & -(\beta+\alpha) & 0 & \beta \\ \alpha & 0 & -(\beta+\alpha) & \beta \\ 0 & \alpha & \alpha & -2\beta \end{pmatrix}, \tag{5.20}$$

and the 3×3 reduced matrix $\widehat{\mathcal{A}}$ is

$$\widehat{\mathcal{A}} = \begin{pmatrix} -(\beta+2\alpha) & -\alpha & \beta-\alpha \\ -\alpha & -(\beta+2\alpha) & \beta-\alpha \\ \alpha & \alpha & -2\beta \end{pmatrix}. \tag{5.21}$$

The latter has the eigenvalues $-\lambda_i$ with $\lambda_1 = \lambda_2 = (\alpha+\beta)$, $\lambda_3 = 2(\alpha+\beta)$, and corresponding eigenvectors

$$\mathbf{e}_1 = \begin{pmatrix} 1 \\ -1 \\ 0 \end{pmatrix}, \quad \mathbf{e}_2 = \begin{pmatrix} \beta-\alpha \\ \beta-\alpha \\ 2\alpha \end{pmatrix}, \quad \mathbf{e}_3 = \begin{pmatrix} 1 \\ 1 \\ -1 \end{pmatrix}. \tag{5.22}$$

Note that $\mathbf{e}_2$ and $\mathbf{e}_3$ are linearly independent since $\alpha, \beta \geq 0$ so that $\beta - \alpha \neq -2\alpha$. We thus have two inverse coherence lengths $\xi_1 = \sqrt{(\alpha+\beta)/D}$ and $\xi_2 = \sqrt{2}\xi_1$.

5.3. Fast switching limit. Intuitively speaking, we might expect the effective single-gate permeability to become independent of N in the fast switching limit $\alpha, \beta \to \infty$, with α/β finite, since spatial correlations vanish. This is most easily established from the switching particle perspective using (5.8). First, we have to specify the rate of switching relative to the diffusion rate over some fundamental length-scale such as the cell length L. Therefore, we introduce the small dimensionless parameter δ according to

$$\delta = \frac{D}{L^2(\alpha+\beta)}.$$

It follows that $\xi L = 1/\sqrt{\delta}$. The fast switching limit is then given by $\delta \to 0$ or, equivalently, $\xi \to \infty$ (for fixed L). Applying this limit to (5.8), we see that

$$\mu_e(N) \to \mu_p \equiv \frac{\mu_0}{\sqrt{\delta}}, \quad \mu_0 = \frac{\rho_0}{2\rho_1}\frac{D}{L}, \tag{5.23}$$

so that the leading-order term is independent of N. Hence, in the fast switching limit, we obtain an N-cell system linked by gap junctions with identical permeability μ_p. We can understand the N-independence of the permeability by noting that the coherence length $\xi^{-1} \to 0$ in the fast switching limit so that spatial correlations between gates become negligible. It is also clear that the permeability diverges as $\delta \to 0$ so that the gap junctions act as open channels, assuming $\rho_0 > 0$. (The same result for a single interior boundary has been obtained in [25].)

The situation from the switching gate perspective is more subtle. Recall from section 3 that we derived the moment equations (3.15) by discretizing space and writing down the CK equation (3.8) for the resulting piecewise deterministic ODE. In order for the spatially discrete model to be a good approximation of the continuum model, we require the switching rates to be slow relative to the time for a particle to diffuse over a lattice spacing a, that is, $D/a^2 \gg \alpha + \beta$. On the other hand, applying a fast switching limit to the CK equation (3.8) requires $D/a^2 \ll \alpha + \beta$. In other words, the continuum and fast switching limits do not commute. Nevertheless, one still finds that in the fast switching limit, the spatially discrete N-cell model can be represented in terms of an array of gap junctions, each having an N-independent permeability μ_G.

In order to establish this result, we set $\alpha = \alpha_0/\varepsilon$ and $\beta = \beta_0/\varepsilon$, with

$$\varepsilon \equiv \frac{D}{a^2(\alpha+\beta)} \ll 1, \tag{5.24}$$

and rewrite the CK equation (3.8) in the form

$$\frac{\partial p_n}{\partial t} = -\sum_{i=1}^{Q} \frac{\partial}{\partial u_i}\left[H_i^n(\mathbf{u})p_n(\mathbf{u},t)\right] + \frac{1}{\varepsilon}\sum_{m=0,1} A_{nm}p_m(\mathbf{u},t), \tag{5.25}$$

with A the matrix (3.9) under $\alpha, \beta \to \alpha_0, \beta_0$, and

$$H_i^n(\mathbf{u}) = \sum_{j=1, j\neq M}^{Q} \Delta_{ij}^n u_j + \eta_a \delta_{i,1}. \tag{5.26}$$

(Equations (3.8) and (5.25) apply to a single gap junction ($N = 2$). However, the analysis easily generalizes to the multicell case; see below.) In the limit $\epsilon \to 0$, one can prove that $p_n(\mathbf{u},t) \to \rho_n\phi(\mathbf{u},t)$ [11] with ϕ satisfying the Liouville equation

$$\frac{\partial \phi}{\partial t} = -\sum_{i=1}^{Q} \frac{\partial}{\partial u_i}\overline{H}_i(\mathbf{u})\phi(\mathbf{u},t),$$

where

$$\overline{H}_i(\mathbf{u}) = \sum_{n=0,1} H_i^n(\mathbf{u})\rho_n. \tag{5.27}$$

Assuming deterministic initial conditions, the Liouville equation is equivalent to the deterministic mean-field equation

$$\frac{du_i}{dt} = \overline{H}_i(\mathbf{u}) = \sum_{j=1}^{M-1} \overline{\Delta}_{ij} u_j + \sum_{j=M+1}^{Q} \overline{\Delta}_{ij} u_j + \frac{\eta D}{a^2}\delta_{i,1}, \tag{5.28}$$

with $\overline{\Delta}_{ij} = \sum_{n=0,1} \rho_n \Delta^n_{ij}$. Away from the interior boundary, $\overline{\Delta}_{ij} = \Delta_{ij}$ with Δ_{ij} given by the discrete Laplacian (3.6a) in the bulk and (3.6b) at the exterior boundaries. At the interior boundary, we find that

$$\overline{\Delta}_{M-1,j} = \frac{D}{a^2}[\delta_{M-2,j} + (\rho_0/2 + \rho_1)\delta_{M-2,j} + (\rho_0/2)\delta_{M+2,j} - 2\delta_{M-1,j}] \tag{5.29a}$$

and

$$\overline{\Delta}_{M+1,j} = \frac{D}{a^2}[\delta_{M+2,j} + (\rho_0/2)\delta_{M-2,j} + (\rho_0/2 + \rho_1)\delta_{M+2,j} - 2\delta_{M+1,j}]. \tag{5.29b}$$

These translate to the following interior boundary conditions:

$$u^-_M = (\rho_0/2 + \rho_1)u_{M-2} + (\rho_0/2)u_{M+2}, \tag{5.30a}$$

$$u^+_M = (\rho_0/2 + \rho_1)u_{M+2} + (\rho_0/2)u_{M-2}. \tag{5.30b}$$

Equation (5.30a) and (5.30b) imply that the spatially discretized flux J through the gap junction is continuous,

$$J = \frac{D}{2a}[u_{M-2} - u^-_M] = \frac{D}{2a}[u^+_M - u_{M+2}] = \frac{\rho_0}{2}[u_{M-2} - u_{M+2}], \tag{5.31}$$

whereas there is a jump discontinuity in the concentration at the gap junction as follows:

$$u^-_M - u^+_M = \rho_1[u_{M-2} - u_{M+2}]. \tag{5.32}$$

For the spatially discrete system we define the permeability according to

$$J = \mu_G[u^-_M - u^+_M], \tag{5.33}$$

and we find that

$$\mu_G = \frac{D}{4a}\frac{\rho_0}{\rho_1}, \tag{5.34}$$

which diverges in the continuum limit $a \to 0$. Although this result was derived in the case of a single gap junction ($N = 2$), it is straightforward to show that the same interior boundary conditions hold at each gap junction when $N > 2$. Hence, in the fast switching limit, the spatially discretized system acts like a deterministic N-cell system with N-independent single-gate permeability μ_G.

In the regime $0 < \epsilon \ll 1$, there are typically a large number of transitions between the discrete states $n = 0, 1$, while $\mathbf{u}$ hardly changes at all. This suggests that the system rapidly converges to the above deterministic solution, which will then be perturbed as $\mathbf{u}$ slowly evolves. The resulting perturbations can be analyzed using a quasi–steady-state (QSS) diffusion or adiabatic approximation, in which the CK equation (5.25) is approximated by a Fokker–Planck (FP) equation for the total density

$\phi(\mathbf{u},t)=\sum_n p_n(\mathbf{u},t)$. The QSS approximation was first developed from a probabilistic perspective by Papanicolaou [33]; see also [16]. It has subsequently been applied to a wide range of problems in biology, including bacterial chemotaxis [19], wave-like behavior in models of slow axonal transport [36, 15], and molecular motor-based models of random intermittent search [30, 31]. The first step in the QSS reduction is to introduce the decomposition

$$p_n(\mathbf{u},t)=\phi(\mathbf{u},t)\rho_n+\epsilon w_n(\mathbf{u},t), \tag{5.35}$$

with

$$\phi(\mathbf{u},t)=\sum_n p_n(\mathbf{u},t),\quad \sum_n w_n(\mathbf{u},t)=0.$$

Substituting the decomposition of p_n into (4.3a) and (4.3b) yields

$$\begin{aligned}\frac{\partial\phi(\mathbf{u},t)}{\partial t}\rho_n+\epsilon\frac{\partial w_n(\mathbf{u},t)}{\partial t}&=-\sum_{i=1}^{Q}\frac{\partial}{\partial u_i}\left(H_i^n(\mathbf{u})[\phi(\mathbf{u},t)\rho_n+\epsilon w_n(\mathbf{u},t)]\right)\\&\quad+\frac{1}{\epsilon}\sum_{m=0,1}A_{nm}[\phi(\mathbf{u},t)\rho_m+\epsilon w_m(\mathbf{u},t)].\end{aligned} \tag{5.36}$$

Summing both sides of (5.36) with respect to n then gives

$$\frac{\partial\phi(\mathbf{u},t)}{\partial t}=-\sum_{i=1}^{Q}\frac{\partial}{\partial u_i}\left(\overline{H}_i(\mathbf{u})\phi(\mathbf{u},t)\right)-\epsilon\sum_{i=1}^{Q}\frac{\partial}{\partial u_i}\left(\sum_{n=0,1}H_i^n(\mathbf{u})w_n(\mathbf{u},t)\right). \tag{5.37}$$

Substituting (5.37) into (5.36) then gives

$$\begin{aligned}\epsilon\frac{\partial w_n(\mathbf{u},t)}{\partial t}&=-\rho_n\sum_{i=1}^{Q}\frac{\partial}{\partial u_i}\left([H_i^n(\mathbf{u})-\overline{H}_i(\mathbf{u})]\phi(\mathbf{u},t)\right)+\sum_{m=0,1}A_{nm}w_m(\mathbf{u},t)\\&\quad-\epsilon\sum_{i=1}^{Q}\frac{\partial}{\partial u_i}\left(H_i^n(\mathbf{u})w_n(\mathbf{u},t)\right)+\epsilon\rho_n\sum_{i=1}^{Q}\frac{\partial}{\partial u_i}\left(\sum_{m=0,1}H_i^m(\mathbf{u})w_m(\mathbf{u},t)\right).\end{aligned}$$

Introduce the asymptotic expansion

$$w_n\sim w_n^0+\epsilon w_n^1+\epsilon^2 w_n^2+\cdots$$

and collect $O(1)$ terms,

$$\sum_{m=0,1}A_{nm}w_m(x,t)=\rho_n\sum_{i=1}^{Q}\frac{\partial}{\partial u_i}\left([H_i^n(\mathbf{u})-\overline{H}_i(\mathbf{u})]\phi(\mathbf{u},t)\right), \tag{5.38}$$

where we have dropped the superscript on w_n^0. The Fredholm alternative theorem shows that this has a unique solution, after imposing the condition $\sum_n w_n(x,t)=0$. More explicitly, using the fact that $w_0=-w_1$, we find that

$$w_0=-\frac{\rho_0}{\alpha_0+\beta_0}\sum_{i=1}^{Q}\frac{\partial}{\partial u_i}\left([H_i^0(\mathbf{u})-\overline{H}_i(\mathbf{u})]\phi(\mathbf{u},t)\right).$$

Finally, substituting this back into (5.37) and using $w_0 = -w_1$ yields the FP equation

$$\frac{\partial \phi(\mathbf{u},t)}{\partial t} = -\sum_{i=1}^{Q} \frac{\partial}{\partial u_i}\left(\overline{H}_i(\mathbf{u})\phi(\mathbf{u},t)\right) + \frac{\varepsilon\rho_0\rho_1}{\alpha_0+\beta_0}\sum_{i,j=1}^{Q}\frac{\partial}{\partial u_i}[H_i^0(\mathbf{u})-H_i^1(\mathbf{u})]\frac{\partial}{\partial u_j}[H_j^0(\mathbf{u})-H_j^1(\mathbf{u})]\phi(\mathbf{u},t), \tag{5.39}$$

which is of Stratonovich form [16].

It is convenient to convert the PDE into Ito form as follows:

$$\frac{\partial \phi(\mathbf{u},t)}{\partial t} = -\sum_{i=1}^{Q}\frac{\partial}{\partial u_i}\left(X_i(\mathbf{u})\phi(\mathbf{u},t)\right) + \varepsilon\sum_{i,j=1}^{Q}\frac{\partial}{\partial u_i}\frac{\partial}{\partial u_j}D_{ij}(\mathbf{u})\phi(\mathbf{u},t),$$

with drift terms

$$X_i(\mathbf{u}) = \overline{H}_i(\mathbf{u}) + \frac{\varepsilon\rho_0\rho_1}{\alpha_0+\beta_0}\sum_{j=1}^{Q}[H_j^0(\mathbf{u})-H_j^1(\mathbf{u})]\frac{\partial}{\partial u_j}[H_i^0(\mathbf{u})-H_i^1(\mathbf{u})] \tag{5.40}$$

and diffusion matrix

$$D_{ij}(\mathbf{u}) = \frac{\rho_0\rho_1}{\alpha_0+\beta_0}[H_i^0(\mathbf{u})-H_i^1(\mathbf{u})][H_j^0(\mathbf{u})-H_j^1(\mathbf{u})]. \tag{5.41}$$

The corresponding Ito SDE is

$$dU_i = X_i(\mathbf{u})dt + \sqrt{\frac{2\epsilon\rho_0\rho_1}{\alpha_0+\beta_0}}[H_i^0(\mathbf{U})-H_i^1(\mathbf{U})]dW(t), \tag{5.42}$$

where $W(t)$ is a Wiener process with

$$\langle dW(t)\rangle = 0, \quad \langle dW(t)dW(t)\rangle = \delta(t-t')dt\,dt'.$$

Taking the expectation of (5.42) and using the fact that $\langle F(\mathbf{U}(t))dW(t)\rangle = 0$ for an Ito process, the mean concentration $V_i(t) = \langle U_i(t)\rangle$ satisfies the ODE

$$\frac{dV_i(t)}{dt} = X_i(\mathbf{V}). \tag{5.43}$$

Carrying out the same analysis as that in (5.28), we find that the effective permeability of the gap junction is now

$$\mu_G = \frac{D}{4a}\frac{\rho_0}{\rho_1}\frac{1-2\varepsilon\rho_1}{1+2\varepsilon\rho_0}. \tag{5.44}$$

Again, our analysis can be extended to multiple gap junctions ($N > 2$).

6. Discussion. In this paper, we generalized recent work [24, 2] on diffusion in domains with randomly switching exterior boundaries to the case of switching interior boundaries. We considered the particular example of a line of cells connected via stochastically gated gap junctions. Solving the resulting first-order moment equations of the stochastic concentration for $N = 2$, we were able to calculate the mean steady-state concentration and flux, and thus extract the effective permeability of the gap

junction. For $N > 2$ (multiple gap junctions), we showed that the effective single-gate permeability depends on N, and that there are major differences between the case where the gap junctions switch between open and closed states and the case where the individual particles switch conformational states. An analogous result holds for other diffusion problems such as diffusion-limited reactions between diffusing ligands and a fixed receptor, where either the ligands or the target receptor switch between active and inactive states [41, 43, 3].

There are a number of possible extensions of this work. First, there is the development of efficient numerical schemes for solving the rth-order moment equations, which rapidly become unwieldy as r and the number of cells N increase. Second, there is extending the analysis to higher dimensions and more general geometric configurations of cells. For example, in the deterministic case, Keener and Sneyd [21] analyzed the steady-state flux for a line of 2D cells with gap-junctional openings in the connecting edges. Using symmetry arguments, they show how the gap junctions along an edge can be lumped into a single effective junction at the center of each edge, whose relative width characterizes the degree of clustering of the gap junctions (uniform distribution of small gap junctions vs. a few large gap junctions). They find that clustered gap junctions lead to a much smaller effective diffusion coefficient D_e for given gap-junctional permeability μ (see also section 2). There has also been a number of studies conducted regarding the effective diffusion coefficient in tubes with periodically alternating diameters or periodically placed obstacles [28, 29]. Third, there is the interest of experimentalists in extracting biophysical constants such as cytoplasmic diffusivity D and gap-junctional permeability based on measurements of tagged particles such as a fluorescent probe. One of the limitations of the steady-state analysis is that the permeability and diffusivity are effectively lumped together. In the deterministic case, it is possible to solve the time-dependent diffusion equation with internal boundary conditions and to fit the resulting solutions to experimental data in order to obtain estimates of diffusivity and permeability [35]. It would therefore be of interest to develop methods for analyzing the full time-dependent stochastic PDE.

Finally, we have assumed throughout that the underlying equations are linear. However, in order to investigate the effects of switching gap junctions on phenomena such as intercellular calcium waves, it would be necessary to include nonlinear chemical reactions.

Appendix A. Recall that the first-order moment equations (4.3a) and (4.3b) determine the average concentration $\mathbb{E}[u(x,t)]$ for $N = 2$. In order to estimate the effects of fluctuations we need to go to higher orders. Here we sketch the steps in calculating the two-point correlation functions

$$C_n(x,y,t) = \mathbb{E}[u(x,t)u(y,t)1_{n(t)=n}], \tag{A.1}$$

given by

$$\frac{\partial C_0}{\partial t} = D\frac{\partial^2 C_0}{\partial x^2} + D\frac{\partial^2 C_0}{\partial y^2} - \beta C_0 + \alpha C_1, \tag{A.2a}$$

$$\frac{\partial C_1}{\partial t} = D\frac{\partial^2 C_1}{\partial x^2} + D\frac{\partial^2 C_1}{\partial y^2} + \beta C_0 - \alpha C_1. \tag{A.2b}$$

For simplicity, we set $D = 1$ and take both cells to have the same length by setting $l = L$. The two-point correlations couple to the first-order moments via the following

external boundary conditions:

(A.3)
$$C_n(0,y,t)=\eta V_n(y,t),\quad C_n(x,0,t)=\eta V_n(x,t),\quad C_n(x,2L,t)=0=C_n(2L,y,t).$$

To see why these are the correct boundary conditions, note that if $n(t)=0$ and $x=0$, then $u(x,t)=\eta$ with probability one, and thus

$$C_0(L,y,t)=\mathbb{E}[u(L,t)u(y,t)1_{n(t)=0}]=\eta\mathbb{E}[u(y,t)1_{n(t)=0}]=\eta V(y,t).$$

The corresponding boundary conditions at the interior boundaries $x=L$, $0\le y\le 2L$, and $y=L$, $0\le x\le 2L$, are

(A.4a) $$[C_0(x,y,t)]_{x=L^-}^{x=L^+}=0=[C_0(x,y,t)]_{y=L^-}^{y=L^+},$$

(A.4b) $$[\partial_x C_0(x,y,t)]_{x=L^-}^{x=L^+}=0=[\partial_y C_0(x,y,t)]_{y=L^-}^{y=L^+},$$

(A.4c) $$\partial_x C_1(x,y,t)|_{x=L^-}=0=\partial_x C_1(x,y,t)|_{x=L^+},$$

(A.4d) $$\partial_y C_1(x,y,t)|_{y=L^-}=0=\partial_y C_1(x,y,t)|_{y=L^+}.$$

As in the case of the first-moment equations, we can solve for the steady-state correlations explicitly, after defining

$$\lim_{t\to\infty}\mathbb{E}[u(x,t)u(y,t)]=C(x,y)\equiv\sum_{n=0,1}C_n(x,y),$$

where $C_n(x,y)\equiv\lim_{t\to\infty}C_n(x,y,t)$. Adding the pair of equations (A.2a,b) gives

(A.5) $$\frac{\partial^2 C}{\partial x^2}+\frac{\partial^2 C}{\partial y^2}=0,$$

with external boundary conditions

(A.6) $$C(x,0)=\eta V(x),\quad C(0,y)=\eta V(y)=0,\quad C(2L,y)=C(x,2L)=0$$

and internal boundary conditions

(A.7) $$\partial_x C(L^-,y)=\partial_x C(L^+,y)=K(y),\quad \partial_y C(x,L^-)=\partial_x C(x,L^+)=K(x).$$

In order to solve this equation we partition the square $[0,2L]\times[0,2L]$ into four squares, as illustrated in Figure 6.

For the moment let us focus on the domain $[0,L]\times[0,L]$ and consider the trial solution

$$C(x,y)=A(y)\sinh(\lambda x)+B(y)\cosh(\lambda x).$$

Imposing the boundary conditions $C(0,y)=\eta V(y)$ and $\partial_x C(L^-,y)=K(y)$ yields

$$B(y)=\eta V(y),\quad A(y)=\frac{K(y)}{\lambda\cosh(\lambda L)}-\eta V(y)\tanh(\lambda L).$$

Similarly, the trial solution

$$C(x,y)=A(x)\sinh(\lambda y)+B(x)\cosh(\lambda y)$$

satisfies the boundary conditions $C(x,0)=\eta V(x)$ and $\partial_y C(x,L^-)=K(x)$. We can add these two solutions without violating the boundary conditions provided that we

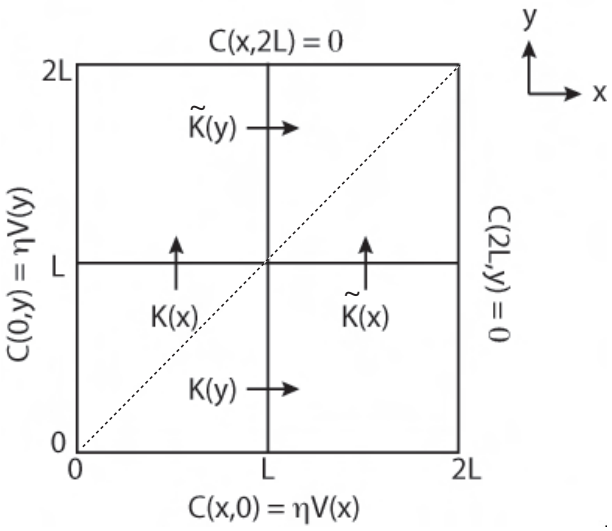

FIG. 6. *Partitioned domain and boundary conditions for the two-point correlation function $C(x,y)$. The solution has a reflection symmetry about the diagonal $x = y$.*

represent the nonperiodic functions as Fourier series such that $V(0) = K(0) = 0$ and $V'(L) = K'(L) = 0$. This can be achieved by setting $\lambda = \lambda_n \equiv (2n+1)\pi/2L$, integer n, and

$$V(z) = \sum_{n\geq 0} V_n \sin(\lambda_n z), \quad K(z) = \sum_{n>0} V_n \sin(\lambda_n z),$$

with

$$V_n = \frac{2}{L}\int_0^L V(z)\sin(\lambda_n z)dz, \quad K_n = \frac{2}{L}\int_0^L K(z)\sin(\lambda_n z)dz.$$

We thus obtain the following solution on $[0,L]\times[0,L]$:

$$\begin{aligned} C(x,y) = {} & \eta\sum_{n\geq 0} V_n\left[\cosh(\lambda_n x) - \tanh(\lambda_n L)\sinh(\lambda_n x)\right]\sin(\lambda_n y) \\ & + \eta\sum_{n\geq 0} V_n\left[\cosh(\lambda_n y) - \tanh(\lambda_n L)\sinh(\lambda_n y)\right]\sin(\lambda_n x) \\ & + \sum_{n\geq 0}\frac{K_n}{\lambda_n\cosh(\lambda_n L)}[\sinh(\lambda_n x)\sin(\lambda_n y) + \sin(\lambda_n x)\sinh(\lambda_n y)]. \end{aligned} \tag{A.8}$$

The next step is to solve (A.2) for C_1 on $[0,L]\times[0,L]$ after setting $C_0 = C - C_1$:

$$\frac{\partial^2 C_1}{\partial x^2} + \frac{\partial^2 C_1}{\partial y^2} - (\alpha+\beta)C_1(x,y) = -\beta C(x,y), \tag{A.9}$$

with

$$C_1(x,0) = \eta V_1(x), \quad C_1(0,y) = \eta V_1(y), \quad \partial_x C_1(L^-,y) = \partial_y C_1(x,L^-) = 0.$$

We can decompose C_1 as

$$C_1(x,y) = \rho_1 C(x,y) + \widehat{C}_1(x,y)$$

such that

$$\frac{\partial^2 \widehat{C}_1}{\partial x^2} + \frac{\partial^2 \widehat{C}_1}{\partial y^2} - (\alpha+\beta)\widehat{C}_1(x,y) = 0, \tag{A.10}$$

with

$$\widehat{C}_1(x,0) = \eta[\rho_0 V_1(x) - \rho_1 V_0(x)], \quad \widehat{C}_1(0,y) = \eta[\rho_0 V_1(y) - \rho_1 V_0(y)],$$

and

$$\partial_x \widehat{C}_1(L^-,y) = -\rho_1 K(y), \quad \partial_y \widehat{C}_1(x,L^-) = -\rho_1 K(x).$$

We can solve the equation for $\widehat{C}_1$ in a similar fashion to C, and the result is

$$\begin{aligned}\widehat{C}_1(x,y) &= \eta \sum_{n\geq 0} \widehat{V}_n \left[\cosh(\mu_n x) - \tanh(\mu_n L)\sinh(\mu_n x)\right]\sin(\lambda_n y) \\ &\quad + \eta \sum_{n\geq 0} V_n \left[\cosh(\mu_n y) - \tanh(\mu_n L)\sinh(\mu_n y)\right]\sin(\lambda_n x) \\ &\quad - \sum_{n\geq 0} \frac{\rho_1 K_n}{\mu_n \cosh(\mu_n L)}[\sinh(\mu_n x)\sin(\lambda_n y) + \sin(\lambda_n x)\sinh(\mu_n y)],\end{aligned} \tag{A.11}$$

where

$$\mu_n^2 = \lambda_n^2 + \alpha + \beta,$$

and $\widehat{V}_n$ are the Fourier coefficients of

$$\widehat{V}(x) = \rho_0 V_1(x) - \rho_1 V_0(x).$$

The solutions in the domain $[0,L]\times[0,L]$ are expressed in terms of the Fourier coefficients K_n of the unknown flux function $K(x)$. We can proceed in a similar fashion to express the solutions in the domain $[L,2L]\times[L,2L]$ in terms of the Fourier coefficients $\widetilde{K}_n$ of $\widetilde{K}(x)$, and the solutions in the domain $[0,L]\times[L,2L]$ (or equivalently the domain $[L,2L]\times[0,L]$) in terms of both K_n and $\widetilde{K}_n$; see Figure 6. Finally, we can determine the Fourier coefficients $K_n, \widetilde{K}_n$ by imposing continuity of $C_0(x,y)$ across the two interior boundaries $L<x<2L, y=L$ and $x=L, 0<y<L$, with

$$C_0(x,y) = \rho_0 C(x,y) - \widehat{C}_1(x,y). \tag{A.12}$$

Acknowledgments. The author would like to thank Sean Lawley for helpful comments regarding the manuscript.

REFERENCES

[1] P. C. Bressloff, *Stochastic Processes in Cell Biology*, Springer, New York, 2004.
[2] P. C. Bressloff and S. D. Lawley, *Moment equations for a piecewise deterministic PDE*, J. Phys. A, 48 (2015), 105001.
[3] P. C. Bressloff and S. D. Lawley, *Stochastically-gated diffusion-limited reactions for a small target in a bounded domain*, Phys. Rev. E., 92 (2015), 062117.
[4] F. K. Bukauskas and V. K. Verselis, *Gap junction channel gating*, Biochim. Biophys. Acta, 1662 (2004), pp. 42–60.
[5] C. C. Chow and J. A. White, *Spontaneous action potentials due to channel fluctuations*, Biophys. J., 71 (1996), pp. 3013–3021.

[6] B. W. Connors and M. A. Long, *Electrical synapses in the mammalian brain*, Ann. Rev. Neurosci., 27 (2004), pp. 393–418.
[7] A. H. Cornell-Bell, S. M. Finkbeiner, M. S. Cooper, and S. J. Smith, *Glutamate induces calcium waves in cultured astrocytes: Long-range glial signaling*, Science, 247 (1990), pp. 470–473.
[8] K. Diba, H. A. Lester, and C. Koch, *Intrinsic noise in cultured hippocampal neurons: Experiment and modeling*, J. Neurosci., 24 (2004), pp. 9723–9733.
[9] A. D. Dorval, *The rhythmic consequences of ion channel stochasticity*, Neuroscientist, 12 (2006), pp. 442–448.
[10] W. J. Evans and P. E. Martin, *Gap junctions: Structure and function*, Mol. Membr. Biol., 19 (2002), pp. 121–136.
[11] A. Faggionato, D. Gabrielli, and M. Ribezzi Crivellari, *Non-equilibrium thermodynamics of piecewise deterministic Markov processes*, J. Stat. Phys., 137 (2009), pp. 259–304.
[12] A. A. Faisal, J. A. White, and S. B. Laughlin, *Ion channel noise places limits on the miniaturization of the brain's wiring*, Curr. Biol., 15 (2006), pp. 1143–1149.
[13] A. A. Faisal, L. P. J. Selen, and D. M. Wolpert, *Noise in the nervous system*, Nat. Rev. Neurosci., 9 (2008), pp. 292–303.
[14] R. F. Fox and Y. N. Lu, *Emergent collective behavior in large numbers of globally coupled independently stochastic ion channels*, Phys. Rev. E, 49 (1994), pp. 3421–3431.
[15] A. Friedman and G. Craciun, *Approximate traveling waves in linear reaction-hyperbolic equations,* SIAM J. Math. Anal., 38 (2006), pp. 741–758, doi:10.1137/050637947.
[16] C. W. Gardiner, *Handbook of Stochastic Methods*, 4th ed., Springer, Berlin, 2009.
[17] J. H. Goldwyn, S. Nikita, M. F. Imennov, M. Famulare, and E. Shea-Brown, *Stochastic differential equation models for ion channel noise in Hodgkin-Huxley neurons*, Phys. Rev. E, 83 (2011), 041908.
[18] D. A. Goodenough and D. L. Paul, *Gap junctions*, Cold Spring Harbor Perspect. Biol., 1 (2009), a002576.
[19] T. Hillen and H. G. Othmer, *The diffusion limit of transport equations derived from velocity-jump processes,* SIAM J. Appl. Math., 61 (2000), pp. 751–775, doi:10.1137/S0036139999358167.
[20] G. A. Jacobson, K. Diba, A. Yaron-Jakoubovitch, Y. Oz, C. Koch, I. Segev, and Y. Yarom, *Subthreshold voltage noise of rat neocortical pyramidal neurons*, J. Physiol., 564 (2005), pp. 145–160.
[21] J. P. Keener and J. Sneyd, *Mathematical Physiology* I: *Cellular Physiology*, 2nd ed., Springer, New York, 2009.
[22] J. P. Keener and J. M. Newby, *Perturbation analysis of spontaneous action potential initiation by stochastic ion channels*, Phys. Rev. E, 84 (2011), 011918.
[23] M. H. Kole, S. Hallermann, and G. J. Stuart, *Single Ih channels in pyramidal neuron dendrites: Properties, distribution, and impact on action potential output*, J. Neurosci., 26 (2006), pp. 1677–1687.
[24] S. D. Lawley, J. C. Mattingly, and M. C. Reed, *Stochastic switching in infinite dimensions with applications to random parabolic PDE*, SIAM J. Math. Anal., 47 (2015), pp. 3035–3063, doi:10.1137/140976716.
[25] S. D. Lawley and J. P. Keener, *A new derivation of Robin boundary conditions through homogenization of a stochastically switching boundary*, SIAM J. Appl. Dyn. Syst., 14 (2015), pp. 1845–1867, doi:10.1137/15M1015182.
[26] L. Leybaert, K. Paemeleire, A. Strahonja, and M. J. Sanderson, *Inositol-trisphosphate-dependent intercellular calcium signaling in and between astrocytes and endothelial cells*, Glia, 24 (1998), pp. 398–407.
[27] L. Leybaert and M. J. Sanderson, *Intercellular Ca^{2+} waves: Mechanisms and function*, Physiol. Rev., 92 (2012), pp. 1359–1392.
[28] Yu. A. Makhnovskii, A. M. Berezhkovskii, and V. Yu. Zitserman, *Time-dependent diffusion in tubes with periodic partitions*, J. Chem. Phys., 131 (2009), 104705.
[29] Yu. A. Makhnovskii, A. M. Berezhkovskii, and V. Yu. Zitserman, *Diffusion in a tube of alternating diameter*, Chem. Phys., 367 (2010), pp. 110–114.
[30] J. M. Newby and P. C. Bressloff, *Quasi-steady state reduction of molecular-based models of directed intermittent search,* Bull. Math. Biol., 72 (2010), pp. 1840–1866.
[31] J. M. Newby and P. C. Bressloff, *Local synaptic signaling enhances the stochastic transport of motor-driven cargo in neurons,* Phys. Biol., 7 (2010), 036004.
[32] J. M. Newby, P. C. Bressloff, and J. P. Keener, *The effect of potassium channels on spontaneous action potential initiation by stochastic ion channels,* Phys. Rev. Lett., 111 (2013), 128101.

[33] G. C. Papanicolaou, *Asymptotic analysis of transport processes,* Bull. Amer. Math. Soc., 81 (1975), pp. 330–392.

[34] N. Paulauskas, M. Pranevicius, H. Pranevicius, and F. F. Bukauskas, *A stochastic four-state model of contingent gating of gap junction channels containing two "fast" gates sensitive to transjunctional voltage*, Biophys. J., 96 (2009), pp. 3936–3948.

[35] S. V. Ramanan and P. R. Brink, *Exact solution of a model of diffusion in an infinite chain or monolayer of cells coupled by gap junctions*, Biophys. J., 58 (1990), pp. 631–639.

[36] M. C. Reed, S. Venakides, and J. J. Blum, *Approximate traveling waves in linear reaction-hyperbolic equations,* SIAM J. Appl. Math., 50 (1990), pp. 167–180, doi:10.1137/0150011.

[37] J. C. Saez, V. M. Berthoud, M. C. Branes, A. D. Martinez, and E. C. Beyer, *Plasma membrane channels formed by connexins: Their regulation and functions*, Physiol. Rev., 83 (2003), pp. 1359–1400.

[38] M. J. Sanderson, A. C. Charles, and E. R. Dirksen, *Mechanical stimulation and intercellular communication increases intracellular Ca^{2+} in epithelial cells*, Cell Regul., 1 (1990), pp. 585–596.

[39] E. Schneidman, B. Freedman, and I. Segev, *Ion channel stochasticity may be critical in determining the reliability and precision of spike timing*, Neural Comput., 10 (1998), pp. 1679–1703.

[40] J. Sneyd, B. T. Wetton, A. C. Charles, and M. J. Sanderson, *Intercellular calcium waves mediated by diffusion of inositol trisphosphate: A two-dimensional model*, Am. J. Physiol. Cell Physiol., 268 (1995), pp. C1537–C1545.

[41] A. Szabo, D. Shoup, S. H. Northrup, and J. A. McCammon, *Stochastically gated diffusion-influenced reactions*, J. Chem. Phys., 77 (1982), pp. 4484–4493.

[42] J. A. White, J. T. Rubinstein, and A. R. Kay, *Channel noise in neurons*, Trends Neurosci., 23 (2000), pp. 131–137.

[43] H.-X. Zhou and A. Szabo, *Theory and simulation of stochastically-gated diffusion-influenced reactions*, J. Phys. Chem., 100 (1996), pp. 2597–2604.